Kinetic Analysis of the RNA-Dependent Adenosinetriphosphatase Activity of DbpA, an *Escherichia coli* DEAD Protein Specific for 23S Ribosomal RNA†

Christopher A. Tsu and Olke C. Uhlenbeck*

Department of Chemistry and Biochemistry, Campus Box 215, University of Colorado, Boulder, Colorado 80309-0215

Received July 31, 1998; Revised Manuscript Received September 22, 1998

ABSTRACT: The adenosinetriphosphatase (ATPase) activity of the *Escherichia coli* DEAD protein DbpA is unusual in that it is specifically stimulated by 23S ribosomal RNA (rRNA). A coupled spectroscopic ATPase assay was used to investigate the interaction of DbpA with RNA and ATP. A 153-base fragment of domain V of 23S rRNA is kinetically identical to intact, native rRNA in activating DbpA: $k_{cat} = 600$ min^{-1}, K_{app}(RNA) = 10 nM, and K_m(ATP) = 120 μM. The ATPase turnover in the absence of RNA is 0.25 min^{-1}. Fragments of 23S rRNA lacking this site (nucleotides 2454−2606) are essentially inactive, as are other RNAs such as poly(A) and tRNA. The relative RNA specificity of DbpA ranges from 10^3 to 10^6 [k_{max}/K_{app}(RNA)]. The interaction with this small RNA fragment was further investigated with regard to stoichiometry, pH, salt and temperature. DbpA is not activated by *E. coli* ribosomes, nor by large subunits, while denatured ribosomes stimulate full ATPase activity. Taken together with the tight, site-specific binding to naked, unmodified 23S rRNA, this suggests a role for DbpA in ribosome biogenesis rather than translation.

The DEAD family of RNA-dependent ATPases is a ubiquitous class of proteins involved in many facets of RNA metabolism, including translation initiation, ribosome biogenesis, pre-mRNA splicing, and mRNA degradation (*1*−*4*). The several hundred family members currently in the database are primarily defined by eight conserved regions, including the namesake Asp-Glu-Ala-Asp (DEAD) sequence, which is a modified form of the Walker B ATP binding motif (*5, 6*). DEAD proteins are members of the second of three loosely related helicase superfamilies (*7*) and share significant homology to the helicase domain of the hepatitis C NS3 (HCV NS3)[1] protein, a well-characterized RNA helicase (*8*−*10*) for which an X-ray cocrystal structure has recently been reported (*11*). While several DEAD proteins have been shown to have ATP-dependent helicase activity *in vitro* with artificial bimolecular substrates (*8*−*10, 12*−*16*), an important challenge of the field is to understand their mechanism of action on natural RNA substrates, where long regions of helical structure do not generally occur.

The role of DEAD proteins *in vivo* has primarily been established by either genetic studies or experiments using crude extracts. Most mechanistic studies performed with several different purified DEAD proteins have been hindered by a lack of substrate specificity. While saturable RNA-dependent ATPase activity can be demonstrated, the activity is fairly insensitive to the type of RNA substrates used (*8, 9, 15*−*17*). Many are active with unstructured homopolymers, and when RNAs believed to be involved in the physiological activity of the DEAD protein are assayed, little (<10-fold) increase in activity is seen (*18, 19*). Similarly, *in vitro* helicase activities do not appear to be sequence-specific *(15, 16*). This lack of specificity is probably due to the absence of additional proteins involved in biological function, but whatever the reason, it makes the mechanistic studies with purified proteins difficult to interpret.

The DEAD protein DbpA from *Escherichia coli* appears to be an attractive candidate for mechanistic studies on this expanding class of proteins. DbpA is one of at least five *E. coli* DEAD proteins (*20, 21*). It was originally identified by its homology to the human DEAD protein P68 (*22*). Cloning and expression of DbpA yielded a highly active RNA-dependent ATPase, with an exceptional specificity for bacterial 23S rRNA (*23, 24*). 16S rRNA, 5S rRNA, tRNA, several homopolymers, and RNAs of eukaryotic origin were all inactive. Subsequent truncation experiments showed that a small fragment of 23S within the peptidyltransferase center was active (*24*), although another group has reported that several additional sites in the rRNA also stimulate DbpA (*25*). Although the physiological function of DbpA is still unknown, the potential for *in vitro* sequence specificity suggests that the correct RNA substrate may have been identified and that additional proteins may not be required for its function.

This paper presents several biochemical experiments on DbpA as a prelude to mechanistic studies. A coupled ATPase assay is used to characterize general properties of

† This work was funded by National Institutes of Health Grants GM37552 and GM36944 to O.C.U. and by a postdoctoral fellowship from The Jane Coffin Childs Memorial Fund for Medical Research to C.A.T.

* To whom correspondence should be addressed: e-mail Olke.Uhlenbeck@Colorado.EDU; Phone 303-492-6929; FAX 303-492-3586.

[1] Abbreviations: HCV NS3, hepatitis C virus nonstructural protein 3; PMSF, phenylmethanesulfonyl fluoride; SDS, sodium dodecyl sulfate; PAGE, polyacrylamide gel electrophoresis; nt, nucleotide; T7, T7 RNA polymerase; PCR, polymerase chain reaction; TLC, thin-layer chromatography; snRNA, small nuclear RNA; snRNP, small nuclear ribonucleoprotein.

10.1021/bi981837y CCC: $15.00
Published on Web 11/11/1998

this activity, to define the sequence specificity, and to identify the major site of action on 23S rRNA. We conclude that DbpA is unlike other biochemically characterized DEAD proteins in several respects and remains a good candidate for understanding how this family of proteins operates.

EXPERIMENTAL PROCEDURES

DbpA Expression. Recombinant DbpA was expressed in BL21(DE3) pLysS cells containing the DbpA pT7.7 plasmid, a generous gift of Frances Fuller-Pace (*23*). Freshly transformed cells were plated on LB-agar containing 50 μg/mL ampicillin and 15 μg/mL chloramphenicol. The bacterial colonies were resuspended from the plate and used to inoculate 2 L of LB medium containing ampicillin and chloramphenicol. These cultures were grown for several hours at 37 °C with shaking until a cell density of approximately 0.3 OD_{600} was reached. At this time, isopropyl β-D-thiogalactopyranoside was added to a concentration of 0.5 mM, and the incubation temperature was reduced to 25 °C. After 4 h, the cells were harvested by centrifugation and stored frozen at −80 °C.

DbpA Purification. DbpA was purified by a modification of the protocols of Frances Fuller-Pace (*23*) and Randall Story (personal communication). Chemicals were from Sigma, except where noted. All procedures were carried out at 4 °C. The frozen cell pellet from 2 L of culture was resuspended in 25 mL of 50 mM Tris, pH 7.5, 100 mM NaCl, 1 mM benzamidine, and 1 mM PMSF (sonication buffer). The cell suspension was sonicated and then clarified by centrifugation at 186000*g* for 1 h. The pellet was resuspended in 25 mL of sonication buffer and centrifuged as above to recover a second DbpA fraction. A $^1/_{10}$ volume of a 2% solution of poly ethyleneimine (Fluka) in 50 mM Tris, pH 7.5, and 100 mM NaCl was added to the pooled supernatants. A white precipitate was removed by centrifuging at 46000*g* for 15 min. The protein was precipitated from the supernatant by addition of ammonium sulfate to 60% and centrifugation at 186000*g* for 15 min. The pellet was resuspended in 10 mL of buffer A (20 mM MOPS, pH 6.8; 50 mM NaCl, and 10% glycerol) plus 1 mM PMSF and dialyzed versus 1 L of buffer A overnight. The dialysate was loaded onto a 16/10 HiLoad SP Sepharose FF column (Pharmacia) equilibrated with buffer A. The column was washed with buffer A until the A_{280} had returned to baseline, and protein was eluted with a 50−1000 mM NaCl gradient in buffer A on a Pharmacia FPLC system. DbpA elutes at ∼350 mM NaCl. At this point, the fraction containing DbpA was >95% pure, as judged by Coomassie-stained SDS−PAGE. The preparation was assayed for nuclease contamination by incubation for 3 h with a radiolabeled RNA oligonucleotide in buffer A at 37 °C. No degradation was observed by denaturing PAGE at DbpA concentrations as high as 4 μM. The protein was concentrated into storage buffer (20 mM MOPS, pH 6.8, 50 mM NaCl, 1 mM DTT, and 50% glycerol) and stored at −80 or −20 °C. DbpA concentration was determined by the molar extinction coefficient calculated from the amino acid sequence, ϵ_{280} = 27 680 M^{-1} cm^{-1} (*26*).

RNA Substrates. Native *E. coli* rRNA (16S and 23S), poly(A) (average length = 10 000 nt), and yeast tRNA were from Boeringer Mannheim. Poly(C) was from Calbiochem. Poly(U) (average molecular weight = 900 000), poly(G), and calf thymus DNA were from Sigma. Total yeast RNA was a generous gift of Irene Ota (University of Colorado). Total *Tetrahymena* RNA was the generous gift of Tom Cech (University of Colorado). Several *E. coli* 23S rRNA substrates were created by runoff transcription with T7 RNA polymerase. Full-length RNA was transcribed from plasmid pCW1 linearized with *Afl*II (nt 1−2904 plus 2 extra adenosine nucleotides) (*27*). Similarly, a series of rRNA fragments, truncated at their 3′ ends, were transcribed after linearization of pCW1 with *Afl*III, *Bsa*HI, *Dra*I, *Eco*RI, *Sal*I, and *Sna*BI. Plasmids encoding domains IV/V (nt 1649−2624) or domain V (nt 2040−2624) were kindly provided by Rachel Green (University of California, Santa Cruz). These RNAs were transcribed after linearization with *Bam*HI. Additional truncated constructs were made from these plasmids by using *Bsa*HI, *Dra*I, or *Pvu*II. The DNA template corresponding to nt 2454−2606, with the necessary T7 promoter, was amplified from pCW1 by PCR and cloned between the *Eco*RI and *Xba*I sites of pUC19. The DNA sequence was verified by dideoxy sequencing. Following linearization with *Xba*I, transcription of this plasmid yielded the 153 nt 2454−2606 fragment, with three additional, nonnative nucleotides on the 3′ end.

RNAs were purified after transcription by acid phenol−chloroform extraction, ethanol precipitation, and G-25 or G-50 size-exclusion chromatography. RNA was stored at −20 °C in 10 mM Tris-HCl, pH 7.5, or 10 mM Hepes-K, pH 7.5. RNA concentrations assume ϵ_{260}= 8600 M^{-1} cm^{-1} $nucleotide^{-1}$. Prior to use, each RNA was refolded in 50 mM Hepes-K, pH 7.5, and 50 mM KCl by heating for 30 s at 100 °C, followed by 90 s at 80 °C, and cooling slowly to room temperature. Full-length native and transcribed rRNAs were refolded in 60 mM Hepes-K, pH 7.5, and 100 mM KCl.

E. coli Ribosomes and 50S Subunits. Tight-couple 70S *E. coli* ribosomes were the generous gift of Mark Welch and Michael Yarus (University of Colorado). *E. coli* ribosome subunits (50S) were kindly provided by Gloria Culver and Harry Noller (University of California, Santa Cruz). Dilutions were made in 20 mM Tris−Cl, pH 7.5, 3 mM DTT, 10 mM magnesium acetate, 100 mM NH_4Cl, and 500 μM EDTA. Ribosomes and subunits were denatured for 15 min at 25 °C after addition of 0.5 M EDTA, pH 8.0, to a final concentration of 0.1 M. A 5 μL aliquot of this mixture was monitored for activity in the standard spectroscopic ATPase assay (see below).

Spectroscopic ATPase Assay. The coupled pyruvate kinase−lactate dehydrogenase assay is a modification of the method described by Bessman (*28*) and Seifried et al. (*29*). Standard buffer conditions were 50 mM Hepes-K, pH 7.5; 50 mM KCl, 5 mM $MgCl_2$, 100 μM DTT, 200 μM NADH, 1 mM phospho(enol)pyruvate, 13−26 μg/mL lactate dehydrogenase, and 23 μg/mL pyruvate kinase. Nucleotide substrates were neutralized with NaOH and were added to reactions in complex with an equimolar amount of $MgCl_2$ ($ATP{\cdot}Mg^{2+}$). Reactions (1 mL volume) were performed in duplicate at 37 °C in a Cary 1E UV−vis spectrophotometer (used with the generous permission of Tom Cech). The oxidation of NADH to NAD^+ was followed at 338 nm (ϵ_{338} = −6220 M^{-1} cm^{-1}). Initial rates and kinetic fits were analyzed with KaleidaGraph (Abelbeck Software). Blank

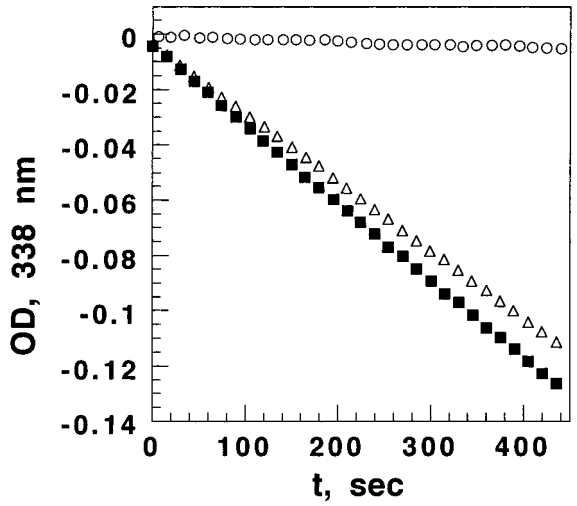

FIGURE 1: rRNA-dependent ATPase activity of DbpA. DbpA (5 nM) was incubated with 2 mM ATP under standard conditions in the absence of RNA (○), 210 nM native rRNA (16S + 23S) (■), or 210 nM 23S rRNA T7 transcript (△).

rates omitting the variable component (ATP or RNA) in kinetic determinations were subtracted from the initial rates. Otherwise, DbpA was omitted from the blank. Background rate of the standard buffer was approximately -1×10^{-5} OD s^{-1} (100 pmol of NADH min^{-1} mL^{-1}) at 37 °C. Error in equation fitting of kinetic parameters was generally less than 10%, with the exception of tRNA $k_{max}/K_{app(RNA)}$ error, which was 30%. Activity differences of protein preparations caused up to 30% batch-to-batch variability in V_{max}. However, each set of experiments was performed with a single protein stock.

TLC ATPase Assay. The release of radioactive phosphate from [γ-^{32}P]ATP was monitored by PEI−cellulose thin-layer chromatography as described by Fuller-Pace et al. (*23*). The reaction conditions were identical to those for the spectroscopic assay minus the coupling reagents [pyruvate kinase, lactate dehydrogenase, phospho(enol)pyruvate, and NADH] and were quenched by the addition of EDTA to 25 mM. TLC plates were quantitated with a Phosphorimager (Molecular Dynamics) after development.

RESULTS

A Coupled ATPase Assay for DbpA. The classic coupled pyruvate kinase−lactate dehydrogenase assay (*28*) was used to monitor ATP hydrolysis by DbpA. This method has been used to study other nucleic acid-dependent ATPases such as Rho (*29*), RecBCD (*30*), and HCV NS3 (*8, 9*). The assay works by coupling ATP hydrolysis to the oxidation of NADH. First, ATP is regenerated from ADP and phospho(enol)pyruvate by pyruvate kinase, producing pyruvate as a product of the reaction. In turn, pyruvate is reduced to lactate by lactate dehydrogenase, with the concomitant oxidation of NADH to NAD^+, which is observed spectroscopically at 338 nm. Figure 1 shows the RNA-dependent ATPase activity of 5 nM DbpA with saturating ATP and *E. coli* rRNA, which gives a turnover number of 540 ATP min^{-1}. The rate is only slightly less (480 min^{-1}) with a synthetic T7 transcript of 23S rRNA. In the absence of RNA, the ATPase rate of DbpA is very low and is obscured in Figure 1 by the buffer background.

Table 1: rRNA Steady-State Kinetic Parameters[a]

RNA	k_{cat} (min^{-1})	K_m(ATP) (μM)	k_{max} (min^{-1})	K_{app}(RNA) (nM)
23S + 16S native	610	235	580	24
23S T7	540	250	530	33
23S 2454−2606	570	120	580	11

[a] Conditions were as described in Figure 2.

The RNA-independent turnover of ATP was determined with several high concentrations of DbpA (up to 2.3 μM and 2 mM ATP). Under these conditions, the measured rate of 0.25 ATP min^{-1} was a linear function of DbpA concentration and was up to 5-fold greater than the buffer background. This rate is ∼2200-fold slower than in the presence of rRNA.

To be sure that the reagents in the coupled assay did not influence the kinetic behavior of DbpA, the assay was corroborated by determining the ATPase activity directly by the release of radioactive phosphate from [γ-^{32}P]ATP (*23*). A limited number of experiments suggest that the maximal activity of DbpA in this uncoupled system is within 2-fold of that determined in the coupled assay (data not shown). Further, the RNA and ATP concentration dependencies of the reaction were similar to those seen with the coupled assay. The TLC assay was also used to show that calf thymus DNA, total yeast RNA, and total *Tetrahymena* RNA do not significantly activate DbpA. These substrates were not characterized further.

Michaelis−Menten Kinetics. It is uncertain whether DbpA performs an irreversible, potentially noncovalent change on rRNA. However, the high rate of ATP hydrolysis with RNA and the very low rate without make it possible to perform the ATPase assay where the DbpA concentration is much less than that of the RNA. Thus, it is appropriate to treat the system as an ATPase with an activating RNA cofactor. This permits two types of experiments to be performed: (1) varying the ATP concentration at saturating RNA, to give k_{cat} and K_m(ATP), using the Michaelis−Menten formalism, and (2) varying the RNA concentration at saturating ATP, to give k_{max} and K_{app}(RNA), the maximal catalytic stimulation and apparent binding constant of the RNA cofactor, respectively.

Data for these experiments with *E. coli* rRNA and the T7 transcript of 23S rRNA are presented in Figure 2, and the kinetic constants are derived in Table 1. From this we make several observations: (1) The K_m(ATP) of 235−250 μM is consistent with that for other DEAD proteins and *E. coli* ATPases (*9, 16, 30*−*32*). (2) Since $k_{cat} = k_{max}$, this indicates that the same E·ATP·RNA complex forms prior to catalysis, regardless of whether full saturation is approached from E·ATP or E·RNA. The order of substrate binding cannot be determined from these experiments. (3) K_{app}(RNA) is quite tight (24−33 nM) and is in a range consistent with other RNA−protein interactions of high specificity (*33*−*35*). (4) All kinetic parameters are very similar for rRNA and the 23S T7 transcript. This suggests that 16S rRNA is not a substrate and that posttranscriptional modifications are not important for the stimulatory activity of 23S rRNA.

Note that these experiments describe only the binding of one ligand in the presence of saturating amounts of the other. It is quite possible that coupling occurs, where the affinity

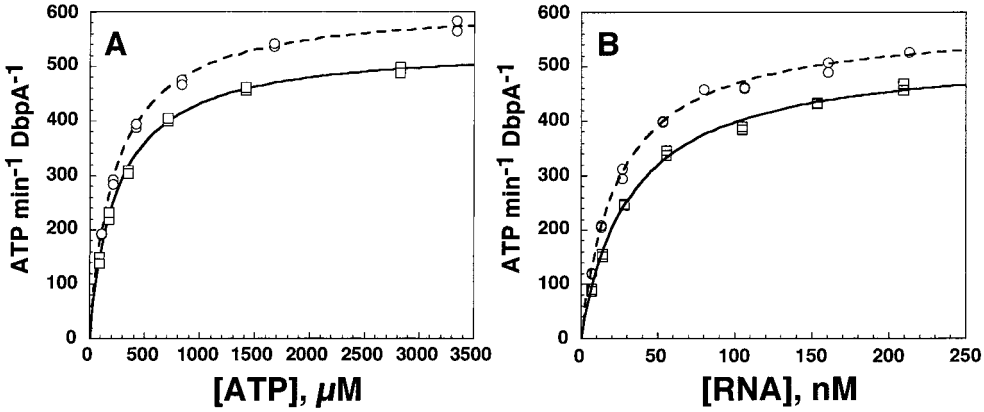

FIGURE 2: Steady-state kinetics of DbpA. *V* versus [S] plots of *E. coli* rRNA (16S + 23S) (○) and 23S rRNA T7 transcript (□), varying either (A) ATP or (B) RNA. The invariant substrate was held at saturating concentrations (2 mM ATP or 160−190 nM RNA), under the standard conditions. The data were fit directly to the Michaelis−Menten equation. The DbpA concentration was in the range of 5−10 nM and was less than the lowest substrate concentration used.

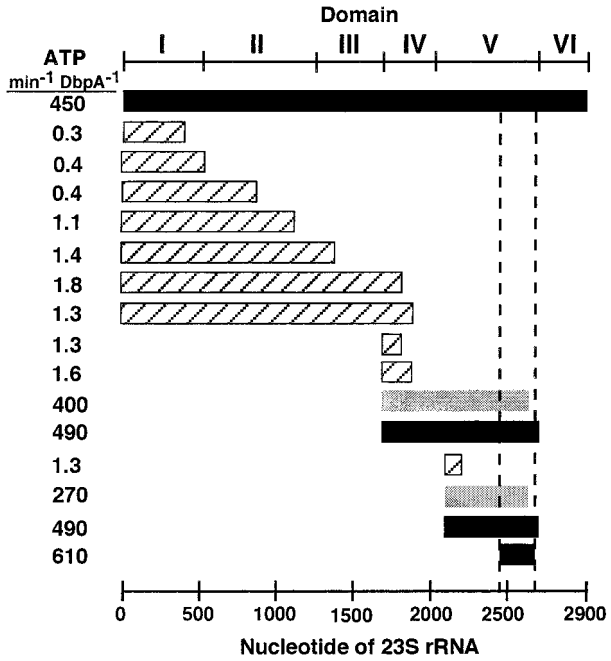

FIGURE 3: ATPase stimulation by 23S rRNA fragments. The 23S rRNA T7 transcript or fragments thereof (150 nM) were assayed under the standard conditions with 2 mM ATP and 5−20 nM DbpA. Fragment shading is representative of ATPase activity: Black indicates full activity (450−610 min^{-1}), gray indicates partial activity (270−400 min^{-1}), and hatched indicates essentially inactive (∼1 min^{-1}). Dotted lines denote the nt 2454−2606 boundary.

of ATP varies as a function of RNA concentration, and vice versa (*36*). Such coupling has been observed for the DEAD protein eIF-4A (*32*). Furthermore, for potentially complex kinetic schemes such as this, the apparent substrate binding constant may not represent the true dissociation constant.

Defining the Binding Site. The high activity of the T7 transcript permits the straightforward generation of fragments of 23S rRNA to define the minimal binding site of DbpA. The experiment was done under conditions that are saturating for the full-length RNA. The data are summarized in Figure 3, superimposed on the linear sequence of 23S rRNA. Regions of the RNA covering domains I−IV show only low levels of activity, not much different than that for nonspecific RNAs (see below). However, there is ∼500-fold higher activity with all fragments that cover nt 2454−2606 (dotted lines in Figure 3). This corroborates in more quantitative fashion the previous finding of Nicol and Fuller-Pace (*24*): one major site for DbpA in 23S rRNA.

Table 2: RNA Specificity of DbpA

RNA	k_{max}/K_{app}(RNA) (min^{-1} nM^{-1})	relative[c]
23S + 16S native[a]	24	2.2
23S T7[a]	16	3.3
23S 2454−2606[a]	53	1
23S 1−1831[b]	0.011	4800
tRNA	0.000036	1500000
poly(A)	0.077	690
poly(U)	0.014	3800
poly(G)	no activity	
poly(C)	no activity	

[a] Derived from Table 1. [b] Substrates of low activity required 25−100 nM DbpA and correspondingly high RNA concentrations for measurement of k_{max}/K_{app}(RNA) under standard conditions (2 mM ATP). [c] [k_{max}/K_{app}(23S 2454−2606)]/[k_{max}/K_{app}(RNA)].

The 153 nt fragment consisting of residues 2454−2606 was examined in greater detail. The kinetic constants show good agreement with the 23S T7 transcript and rRNA (Table 1). The very small differences (2−3-fold) in the RNA and ATP binding constants for the different RNAs most likely reflect heterogeneity in the large rRNA samples. This indicates that the region presumably contains *all* determinants required for stimulation of the ATPase activity. The fragment comprises the lower half of the central wheel of domain V, including cross-link sites for A-, P-, and E-site tRNA (*37*−*39*).

Specificity for RNA. Other RNAs were examined to evaluate the specificity of DbpA. A series of subsaturating RNA concentrations at 25−100 nM DbpA were assayed at 2 mM ATP. The observed rate, corrected for the molar RNA and DbpA concentrations, gives k_{max}/K_{app}(RNA), a quantity that should reflect the differing ability of RNAs to bind to DbpA and stimulate its ATPase activity. The numbers assume only one DbpA binds per RNA, a reasonable assumption, considering that the concentration of DbpA is less than that of the RNA in these experiments. As shown in Table 2, the relative specificity is very high (>600-fold). Most RNAs show only a slight increase over the no-RNA control. Significantly, a large fragment of 23S (nt 1−1831) that does not contain the 2454−2606 binding site is 5000-

fold less active than the nt 2454−2606 RNA. Although Boddeker et al. (*25*) reported high levels of activation of DbpA by three sites within this part of native 23S rRNA, our more quantitative spectroscopic assay suggests that activation by these regions is not greater than that by nonspecific RNA. Furthermore, the presence of several additional sites, nearly equivalent in activity to the main 2454−2606 locus, should have had a noticeable effect on the ATPase kinetics of full-length 23S rRNA substrates. None was seen, even for native rRNA similar to that used in other studies (*24*, *25*). The nonspecific RNAs poly(A) and poly(U) were slightly more active than the nt 1−1831 construct. There are some differences between homopolymers, but all are only weakly stimulatory as compared to the 23S controls. This is probably because they bind poorly to DbpA. Yeast tRNA is among the worst substrates. The compact tertiary structure of tRNA likely prohibits tight binding to DbpA. The relative RNA specificity ranges over 6 orders of magnitude. This speaks to the remarkable selectivity of DbpA, as well as to the sensitivity of the spectroscopic ATPase assay.

Properties of the Reaction. In many cases, *in vitro* biochemical experiments are performed under a set of a few empirically determined reaction conditions. This can, in the least, make it difficult to quantitatively compare different experiments, even those done on the same or similar biomolecules. More fundamentally, essential kinetic and thermodynamic properties of a reaction or macromolecular interaction can be determined by varying the physical conditions of the system. The convenience of the coupled ATPase assay and the high activity and specificity of the 2454−2606 RNA makes such manipulation straightforward. Control experiments with added ADP show that in all of the following experiments, the coupling enzymes are sufficiently active that they do not become rate-limiting.

The pH dependence of the ATPase activity was carried out at saturating ATP and RNA using a series of buffers between pH 5.5 and 9.1. Very little pH dependence is seen between 6.6 and 8.5. This suggests that the chemistry is not rate-limiting for a wide range of conditions. The rate decreases at the higher and lower ends, primarily due to irreversible protein inactivation (data not shown).

The magnesium dependence of the reaction was investigated. As the coupling enzymes require Mg^{2+} for activity, only Mg^{2+} concentrations greater than 0.5 mM could be tested. The rate changed little between 0.5 and 5 mM and then decreased roughly linearly [−25 ATP min^{-1} (mM $MgCl_2)^{-1}$] at higher Mg^{2+} (data not shown). This is likely due to ionic strength effects.

The monovalent ionic strength dependence of the reaction was examined in some detail at varying KCl concentrations. It was found that while both ATP and RNA binding weakened significantly with increasing KCl, the catalytic rate was unaffected (data not shown). Plots of log K_m(ATP) and log K_{app}(RNA) versus log [K^+] gave linear correlations (Figure 4). In accordance with condensation theory of RNA−counterion interactions (*40*), the slopes suggest that 2−3 K^+ are displaced upon RNA binding and 1 upon ATP binding, although this is complicated by the presence of Mg^{2+} and other salts.

The temperature dependence of the reaction was determined under conditions of saturating 2454−2606 RNA (150 nM) and ATP (2 mM) in the standard buffer. The reaction rate increased exponentially from 24 ATP min^{-1} to 1100 ATP min^{-1} as the temperature was increased from 5 to 42 °C (data not shown). The Eyring plot of ln (kh/k_bT) versus T^{-1} is slightly curved, but $\Delta H^‡$ (70 ± 2.7 kJ mol^{-1}) and $\Delta S^‡$ (3.7 ± 9.7 J mol^{-1} K^{-1}) can be calculated. The transition-state parameters suggest a modest activation energy with little change in entropy in the system.

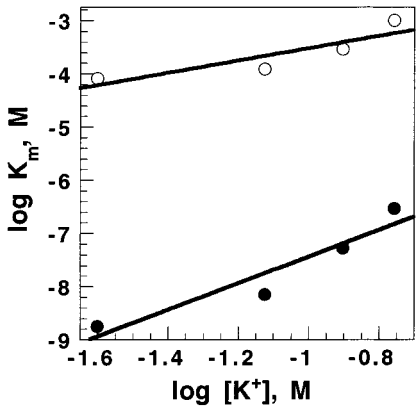

FIGURE 4: Monovalent salt dependence of substrate binding. DbpA (10 nM) was incubated with 150 nM 2454−2606 RNA and 2 mM ATP in the standard buffer where the KCl concentration was varied. A base level of 25 mM K^+ is contributed by the buffer. [K^+] dependence of K_m(ATP) (○) and K_{app}(RNA) (●) is plotted. Slope of the ATP fit is 1.2 ± 0.4; slope of the RNA fit is 2.5 ± 0.6.

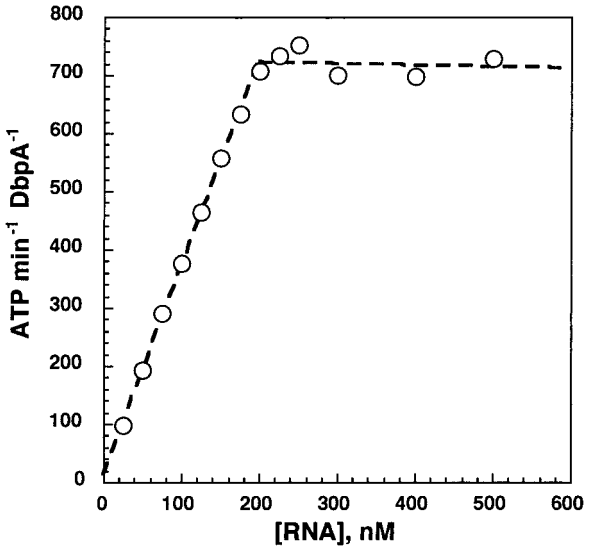

FIGURE 5: Stoichiometry of DbpA·2454−2606 RNA complex. DbpA (180 nM) was titrated with 25 nM aliquots of 2454−2606 RNA in modified standard buffer (3 mM $MgCl_2$) and 2 mM ATP. Points represent the average of two determinations.

Stoichiometry of DbpA for RNA. The 2454−2606 RNA fragment was used to determine the stoichiometry of the RNA−protein complex. The experiment was performed at 180 nM DbpA, which is 15-fold higher than the K_{app}(RNA). Thus, any added RNA will be bound completely until the protein is saturated. Similarly, subtleties of the RNA−protein interaction, such as cooperative binding, cannot be determined under these conditions. As shown in Figure 5, the ATPase activity of DbpA increases linearly with added RNA, until a break is observed at 200 nM, indicating equimolar stoichiometry. The maximal ATPase rate of 700 min^{-1} is in good agreement determined under conditions of

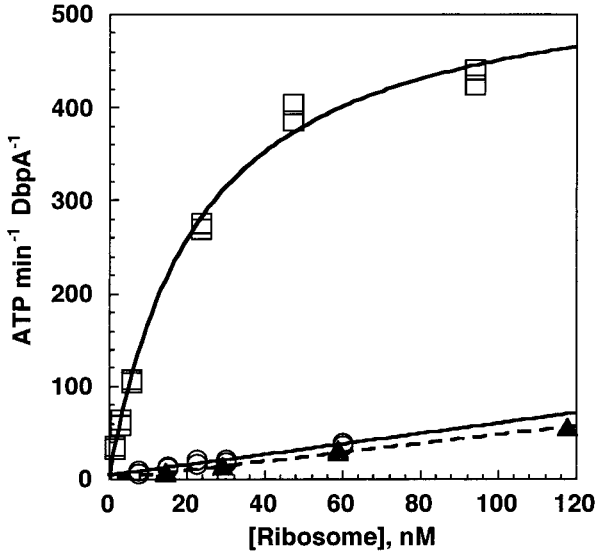

FIGURE 6: ATPase stimulation by ribosomes and EDTA denatured ribosomes. DbpA (5−10 nM) was incubated in the standard buffer (2 mM ATP) with several concentrations of 70S tight-couple ribosomes (○), purified 50S subunits (▲), or EDTA-denatured 70S ribosomes (□).

Table 3: Kinetic Parameters for Ribosome Substrates[a]

substrate	k_{max} (min^{-1})	K_{app}(RNA) (nM)	k_{max}/K_{app}(RNA) (min^{-1} nM^{-1})
70S ribosomes			0.47
50S subunits			0.56
70S + EDTA	550	23	24
23S + 16S rRNA[b]	580	24	24

[a] Conditions were as described in Figure 6. [b] Data from Table 2.

trace DbpA and RNA excess (Figure 2). This experiment suggests that at RNA saturation the complex consists of one molecule each of protein and RNA, but further characterization is needed. The high protein concentration used (180 nM) makes it possible that more than one molecule of DbpA may bind to the RNA, especially at low RNA concentrations. Although we have observed multiple, nonspecific binding of DbpA to the 2454−2606 RNA under similar conditions by gel-shift methods (data not shown), such interactions do not appear to activate DbpA in the coupled ATPase assay. Also, nonspecific binding is likely to be relatively weak and easily competed against, as the ATPase activity increases linearly with the 2454−2606 RNA concentration. Further investigation of the oligomeric state of DbpA is warranted, as this has been critical in elucidating mechanisms of related classes of enzymes, such as helicases and other motor proteins (*41*).

Activity with Ribosomes. It was of great interest to see whether DbpA interacts with mature ribosomes. The ATPase rate was measured at 2 mM ATP, 5−10 nM DbpA, and several concentrations of either 70S tight-couple ribosomes or purified 50S subunits. As shown in Figure 6 and Table 3, the activity is very low, 50−100-fold lower than the 23S rRNA controls. The slightly higher rate for the 50S subunits may reflect the presence of small amounts of partially denatured ribosomes. Indeed, control experiments where the ribosomes or 50S subunits were disrupted by treatment with 100 mM EDTA (*42*) prior to assay gave full ATPase activity (Figure 6 and data not shown). Remarkably, the kinetic constants for the EDTA-treated ribosomes were identical to those for naked rRNA (Table 3). These data clearly suggest that the mature ribosome is not an active substrate for DbpA.

Table 4: Kinetic Parameters of DEAD Proteins

protein	+RNA k_{cat} (min^{-1})	−RNA k_{cat} (min^{-1})	activation factor[a]	K_{app}(RNA) (nM)	K_mATP (μM)	ref
DbpA	600	0.25	2400	11	120	
eIF-4A	1[b]	0.002	500	1000	10	*32*
	3[c]	0.006		125 000	330	
PRP5	440			570		*19*
PRP16	90	9	10			*17*
PRP22	400	100	4		95	*16*
HCV NS3	2200	200	11	290−1500	95	*9*

[a] (+RNA k_{cat})/(−RNA k_{cat}). [b] pH 6.0. [c] pH 7.4.

DISCUSSION

Kinetic Comparison of DbpA and Other DEAD Proteins. The kinetic experiments performed in this study are presented in comparison with those of other DEAD proteins (Table 4). Although it is likely that these proteins hydrolyze ATP by a conserved mechanism (*5, 6, 43*), the data reflect more closely the functional diversity of this family. The ATPase k_{cat} is variable, with DbpA being among the faster enzymes. The weak ATPase activity of several proteins may reflect low intrinsic catalytic activity, the stimulatory ability of the RNA, or lack of protein cofactors. The degree to which the ATPase is stimulated by RNA is variable, ranging from 10 to 1000-fold. This appears to reflect inherent properties of the individual proteins, such as the basal level of ATP hydrolysis, as well as more general issues of substrate recognition and catalysis. One notes that the absolute ATPase activity of DbpA versus nonspecific RNA substrates is low and resembles that of other DEAD proteins, especially eIF-4A.

The apparent RNA binding constants vary widely, and excepting DbpA, are rather weak (∼0.5−100 μM). It is likely that the artificial, homopolymeric nature of most of the RNA substrates is a contributing factor, as many DEAD proteins are known to catalyze specific tasks *in vivo*. Interestingly, PRP5, which shows some specificity for U2 snRNA (∼10-fold), binds to this RNA weakly (>500 nM) (*19*). This may reflect the cellular abundance of the U2 snRNA (*44*), or that the intact snRNP particle may be the actual substrate for PRP5.

In contrast, the RNA binding of DbpA is tight (∼10 nM) and similar to that observed for other RNA−protein interactions, such as aminoacyl-tRNA synthetases (*45*, *46*), cyt-18 protein/group I intron (*33*), MS2 coat protein/viral RNA (*34*), and ribosomal protein S15/16S rRNA (*47*). Strikingly, DbpA exhibits an RNA specificity of at least 500-fold. That the DbpA−rRNA interaction responds predictably to such physical reaction parameters as pH, temperature, and ionic strength suggests the system is robust. DbpA is an exceptional DEAD protein, well suited for further mechanistic studies.

Is RNA a Cofactor or a Substrate for DbpA? In this work, we have considered RNA a cofactor rather than a substrate of DbpA. This is because we have found no evidence for any change in the ability of the RNA to stimulate ATPase activity, even after prolonged incubation with DbpA. For example, under conditions of saturating, excess DbpA where

all the RNA is bound to protein, the ATP hydrolysis rate is extremely high, 700 ATP min^{-1} per RNA molecule, and remains unchanged for at least 7 min (Figure 5 and unpublished results). This represents a cumulative turnover of 5000 ATP for each RNA molecule in the assay. A rate constant for the dissociation of RNA from DbpA can be estimated to be between 1 and 10 min^{-1}, based upon a K_{app}-(RNA) of 10 nM and assuming $k_{on} = 10^8-10^9$ min^{-1} M^{-1} (*48*). This suggests that an average of 70 ATP molecules are hydrolyzed before the RNA molecule is released from the protein. If DbpA catalyzes an ATP-dependent structural isomerization, it must be inefficient and readily reversible. It is possible, of course, that when DbpA acts in its physiological setting, additional components could trap a product that has only a short lifetime *in vitro.* This is consistent with the observation that DbpA is stimulated continually by naked 23S rRNA but not at all by mature, assembled ribosomes.

The rRNA Site Is Suggestive of Biological Functions for DbpA. The binding site of DbpA is quite interesting. This DEAD protein is specifically activated by a fragment of the peptidyltransferase center of 23S rRNA (nt 2454−2606). In particular, this region comprises several helical domains and has been implicated in A-, P-, and E-site tRNA binding by a variety of methods (*37, 39, 49, 50*). Chemical modification data suggests that this RNA is structured and relatively accessible to solvent in the ribosome (Harry F. Noller, personal communication). Other experimental and computational analyses suggest that this part of domain V may fold into a complex structure with domains IV and VI (*37, 51*). Ribosomal protein L6 cross-links to nt 2473−2481 within the DbpA site (*52*). Other proteins, including L1, L13, L16, L32, and L33, are also located nearby, though the degree of protein binding to the central structural elements of the site (nt 2507−2582) is unknown (*37, 38, 53*). It is quite conceivable that DbpA might aid in the assembly or modulation of higher-order structure of this critical region of the ribosome.

Although no physiological data is yet available, one can use these biochemical results to speculate about the function of DbpA. Its low abundance in *E. coli* (*22*) and its very high affinity for 23S rRNA in vitro suggest that it must act on a form of rRNA that is present in low intracellular concentration. Though the concentration of rRNA inside *E. coli* has been estimated to be as high as 35 μM (*54*), most is in the form of ribosomes, which do not appear to interact with DbpA. While it remains possible that DbpA interacts with a minor component of ribosomes, a more attractive possibility is that DbpA has a role in ribosome biogenesis. Since DbpA is fully active on 23S transcripts, it may act at an early stage of assembly. Interestingly, at least six posttranscriptional modifications have been identified in native rRNA within the nt 2454−2606 DbpA binding site (*55*). A subset of these modifications are required for proper *in vitro* assembly and function of the 50S ribosomal subunit (*56*). Apparently, none are critical for DbpA activity.

ACKNOWLEDGMENT

We thank Karl Kossen and Alexey Wolfson for many stimulating discussions and a careful reading of the manuscript. We also thank Evelyn Jabri for her comments on the manuscript. We acknowledge Randall Story and Frances Fuller-Pace for their substantial support of this work.

REFERENCES

1. Pause, A., and Sonnenberg, N. (1993) *Curr. Opin. Struct. Biol. 3*, 953−959.
2. Schmid, S., and Linder, P. (1992) *Mol. Microbiol. 6*, 283−292.
3. Wassarman, D., and Steitz, J. (1991) *Nature 349*, 463−464.
4. Jacobs Anderson, J., and Parker, R. (1996) *Curr. Biol. 6*, 780−782.
5. Yoshida, M., and Amano, T. (1995) *FEBS Lett. 359*, 1−5.
6. Walker, J., Saraste, M., Runswick, M., and Gay, N. (1982) *EMBO J. 1*, 945−951.
7. Gorbalenya, A., and Koonin, E. (1993) *Curr. Opin. Struct. Biol. 3*, 419−429.
8. Morgenstern, K. A., Landro, J. A., Hsiao, K., Lin, C., Gu, Y., Su, M. S., and Thomson, J. A. (1997) *J. Virol. 71*, 3767−3775.
9. Preugschat, F., Averett, D. R., Clarke, B. E., and Porter, D. (1996) *J. Biol. Chem. 271*, 24449−24457.
10. Porter, D., Short, S. A., Hanlon, M. H., Preugschat, F., Wilson, J. E., Willard, D. J., and Consler, T. G. (1998) *J. Biol. Chem. 273*, 18906−18914.
11. Kim, J., Morgenstern, K., Griffith, J., Dwyer, M., Thomson, J., Murcko, M., Lin, C., and Caron, P. (1998) *Structure 6*, 89−100.
12. Hirling, H., Scheffner, T., and Stahl, H. (1989) *Nature 339*, 562−564.
13. Shuman, S. (1992) *Proc. Natl. Acad. Sci. U.S.A. 89*, 10935−10939.
14. Pause, A., and Sonenberg, N. (1992) *EMBO J. 11*, 2643−2654.
15. Wang, Y., Wagner, J. D. O., and Guthrie, C. (1998) *Curr. Biol. 8*, 441−451.
16. Wagner, J. D., Jankowsky, E., Company, M., Pyle, A. M., and Abelson, J. N. (1998) *EMBO J. 17*, 2926−2937.
17. Schwer, B., and Guthrie, C. (1992) *Mol. Cell. Biol. 12*, 3540−3547.
18. Xu, D., Nouraini, S., Field, D., Tang, S. J., and Friesen, J. D. (1996) *Nature 381*, 709−713.
19. O'Day, C., Dalbadie-McFarland, G., and Abelson, J. (1996) *J. Biol. Chem. 271*, 33261−33267.
20. Ohmori, H. (1994) *Jpn. J. Genet. 69*, 1−12.
21. Reuven, N. B., Koonin, E. V., Rudd, K. E., and Deutscher, M. P. (1995) *J. Bacteriol. 177*, 5393−5400.
22. Iggo, R., Picksley, S., Southgate, J., McPheat, J., and Lane, D. P. (1990) *Nucleic Acids Res. 18*, 5413−5417.
23. Fuller-Pace, F., Nicol, S., Reid, A., and Lane, D. (1993) *EMBO J. 12*, 3619−3626.
24. Nicol, S., and Fuller-Pace, F. (1995) *Proc. Natl. Acad. Sci. U.S.A. 92*, 11681−11685.
25. Boddeker, N., Stade, K., and Franceschi, F. (1997) *Nucleic Acids Res. 25*, 537−545.
26. Gill, S. C., and von Hippel, P. H. (1989) *Anal. Biochem. 182*, 319−326.
27. Weitzmann, C. J., Cunningham, P. R., and Ofengand, J. (1990) *Nucleic Acids Res. 18*, 3515−3520.
28. Bessman, M. (1963) *Methods Enzymol. 6*, 166−176.
29. Seifried, S. E., Wang, Y., and von Hippel, P. H. (1988) *J. Biol. Chem. 263*, 13511−1354.
30. Roman, L. J., and Kowalczykowski, S. C. (1989) *Biochemistry 28*, 2873−2881.
31. Reinstein, J., Schlichting, I., and Wittinghofer, A. (1990) *Biochemistry 29*, 7451−7459.
32. Lorsch, J. R., and Herschlag, D. (1998) *Biochemistry 37*, 2180−2193.
33. Guo, Q., and Lambowitz, A. M. (1992) *Genes Dev. 6*, 1357−1372.
34. LeCuyer, K. A., Behlen, L. S., and Uhlenbeck, O. C. (1996) *EMBO J. 15*, 6847−6853.
35. Pingoud, A., Reisner, D., Boehme, D., and Maass, G. (1973) *FEBS Lett. 30*, 1−5.

36. Segel, I. (1975) *Enzyme Kinetics*, pp 227−231, John Wiley and Sons, New York.
37. Zimmermann, R. A., Thomas, C. L., and Wower, J. (1990) in *The Ribosome: Structure, Function and Evolution* (Hill, W. E., Dahlberg, A., Garrett, R., Moore, P. B., Schlessinger, D., and Warner, J. R., Ed.) 331−347, American Society for Microbiology, Washington, DC.
38. Baranov, P. V., Sergiev, P. V., Dontsova, O. A., Bogdanov, A. A., and Brimacombe, R. (1998) *Nucleic Acids Res. 26*, 187−189.
39. Green, R., Switzer, C., and Noller, H. F. (1998) *Science 280*, 286−289.
40. Record, M. J., Anderson, C., and Lohman, T. (1978) *Q. Rev. Biophys. 11*, 103−178.
41. Lohman, T. M., Thorn, K., and Vale, R. D. (1998) *Cell 93*, 9−12.
42. King, T. C., Rucinsky, T., Schlessinger, D., and Milanovich, F. (1981) *Nucleic Acids Res. 9*, 647−661.
43. Saraste, M., Sibbald, P. R., and Wittinghofer, A. (1990) *Trends Biochem. Sci. 15*, 430−434.
44. Zieve, G. W. (1981) *Cell 25*, 296−297.
45. Pingoud, A., Boehme, D., Riesner, D., Knownatski, R., and Maass, G. (1975) *Eur. J. Biochem. 56*, 617−622.
46. Krauss, G., Römer, R., Riesner, D., Boehme, D., and Maass, G. (1973) *FEBS Lett. 30*, 6−9.
47. Batey, R. T., and Williamson, J. R. (1996) *J. Mol. Biol. 261*, 536−549.
48. Fersht, A. (1985) *Enzyme Structure and Mechanism*, pp 150−151, W. H. Freeman, New York.
49. Joseph, S., Weiser, B., and Noller, H. F. (1997) *Science 278*, 1093−1098.
50. Rinke, A. J., Junke, N., Osswald, M., and Brimacombe, R. (1995) *RNA 1*, 1018−1028.
51. Gutell, R. (1996) in *Ribosomal RNA: Structure, Evolution, Processing, and Function in Protein Biosynthesis* (Zimmermann, R. A., and Dahlberg, A. E., Eds.) pp 111−128, CRC Press, Boca Raton, FL.
52. Osswald, M., Greuer, B., and Brimacombe, R. (1990) *Nucleic Acids Res. 18*, 6755−6760.
53. Muralikrishna, P., and Cooperman, B. S. (1995) *Biochemistry 34*, 115−121.
54. Pang, H., and Winkler, H. H. (1994) *Mol. Microbiol. 12*, 115−120.
55. Kowalak, J. A., Bruenger, E., and McCloskey, J. A. (1995) *J. Biol. Chem. 270*, 17758−17764.
56. Green, R., and Noller, H. F. (1996) *RNA 2*, 1011−1021.

BI981837Y